Cancer Science
The official journal of the Japanese Cancer Association

Conditionally replicative adenoviral vectors for imaging the effect of chemotherapy on pancreatic cancer cells

Jun Kimura,[1] Hidetaka A. Ono,[1] Takashi Kosaka,[1] Yoji Nagashima,[2] Shuichi Hirai,[3] Shigeo Ohno,[3] Kazunori Aoki,[4] Davydova Julia,[5] Masato Yamamoto,[5] Chikara Kunisaki[1,6] and Itaru Endo[1]

Departments of [1]Gastroenterological Surgery; [2]Molecular Pathology; [3]Molecular Biology, Graduate School of Medicine, Yokohama-city University, Yokohama; [4]Division of Gene and Immune Medicine, National Cancer Center Research Institute, Tokyo, Japan; [5]Division of Basic and Translational Research, Department of Surgery, University of Minnesota, Minneapolis, Minnesota, USA

(Received February 13, 2013/Revised May 1, 2013/Accepted May 3, 2013/Accepted manuscript online May 16, 2013/Article first published online July 3, 2013)

Pancreatic cancer has a poor prognosis after complete macroscopic resection combined with chemotherapy. Even after neoadjuvant chemotherapy, R0 resection is often not possible. Moreover, current imaging techniques cannot reliably distinguish viable cancer cells from scar tissue at the resectional margin. We investigated the use of a conditionally replicative adenovirus (CRAd), Ad5/3Cox2CRAd-ΔE3ADP-Luc, for imaging the effects of chemotherapy. The CRAd infectivity of pancreatic cancer cells was enhanced by a chimeric Ad5/3 fiber, E1A expression was under the control of the Cox2 promoter, and the luciferase gene was inserted adjacent to the adenovirus death protein (*ADP*) gene. Subcutaneous xenografts of the pancreatic cancer cell line MiaPaCa-2 were established in 24 BALB/c nu/nu mice. When xenografts reached a diameter of 4–6 mm (day 1), the mice were injected i.p. with either PBS (group A; $n = 12$) or 1000 mg/kg gemcitabine (group B; $n = 12$), weekly. On days 19, 26, 33, and 40, CRAd were injected intratumorally into three mice in groups A and B. Bioluminescence was imaged 72 h after CRAd injection, and gross tumor volumes were measured then tumors were removed for *ex vivo* histopathology using H&E and Ki-67 staining. Correlations between gross tumor volume, pathological evaluation of the percentage of viable tumor area, and CRAd bioluminescence were analyzed. Bioluminescence correlated closely with the percentage of viable tumor area ($R = 0.96$), but not with gross tumor volume ($R = 0.31$). Therefore, CRAds might be reliable imaging tools for monitoring chemotherapy in pancreatic cancer, and could improve our ability to distinguish viable tumor cells from scar tissue. (*Cancer Sci* 2013; 104: 1083–1090)

Pancreatic adenocarcinoma has one of the worst survival rates of all cancers worldwide, with only a 5% five-year survival rate, for all stages. In 2008, 37 680 new cases of pancreatic cancer were diagnosed, and 34 290 deaths were expected.[1] In Japan, only 20% of patients diagnosed with pancreatic cancer are treatable by resection, as 50–60% of patients already have distant metastases and approximately 30% of patients have locally advanced disease that is not resectable.[2] Median survival rates of 20–24 months can be expected only in cases where resection is possible and is combined with postoperative chemotherapy or chemoradiation.[3–5] However, two-thirds of patients that are borderline resectable and one-third of patients that are clinically unresectable could become resectable after neoadjuvant therapy, resulting in a prognosis comparable to those patients with resectable tumors.[2] Several reports[6–11] have suggested that the number of patients with unresectable or borderline resectable pancreatic cancer for whom a microscopic tumor clearance (R0) resection becomes possible will increase as new aggressive regimens such as FOLFIRINOX[12,13] are developed.

When using such therapeutic strategies, it is important to establish whether remnant cancer cells exist at resectional margins after neoadjuvant therapy. However, current techniques for cross-sectional imaging, including PET-CT, cannot reliably distinguish viable cancer cells from scar tissue because the increased soft-tissue density observed around celiac or superior mesenteric arteries after neoadjuvant therapy is often scar tissue without viable tumor cells.[14,15] As it is not possible to evaluate the effects of chemotherapy on pancreatic cancer based on residual tumor volume (gross tumor volume), it is difficult to determine whether surgery is indicated after neoadjuvant therapy in patients with a stable tumor volume. Thus, novel imaging tools are urgently needed to distinguish viable cancer cells from scar tissue in pancreatic cancer.

Conditionally replicative adenoviruses have been designed to replicate only in cancer cells, and have been developed mainly as cancer therapeutics.[16,17] Clinical trials in cancers including pancreatic, prostate, ovarian, and glioblastoma multiforme,[18,19] have established that CRAds are tolerated. Previous studies in mouse models found that CRAds are excellent tools for the non-invasive imaging of cancer cells, and can be specifically cytocidal.[20,21] Furthermore, CRAd(Ad5/3Cox2-CRAd-ΔE3-ADP-Luc) has been specifically developed to infect viable pancreatic cancer cells, replicate in them, and emit light.[22–25] This CRAd shows promising characteristics for use both *in vitro* and *in vivo*; however, it has so far not been evaluated as a diagnostic for assessing the effects of chemotherapy. The current study investigated whether CRAd(Ad5/3Cox2-CRAd-ΔE3-ADP-Luc) was a useful imaging tool for monitoring the effects of chemotherapy on pancreatic cancer.

Materials and Methods

Cell lines and cell culture. The MiaPaCa-2, BxPC-3, and Panc-1 pancreatic cancer cell lines (ATCC, Manassas, VA, USA) and the Cox2-positive lung cancer cell line A549 (JCRB0076; Health Science Research Resources Bank, Osaka, Japan) were grown in DMEM with 10% FCS (JRH Biosciences, Lenexa, KS, USA). The Cox2-negative breast cancer cell line BT-474 (THB-20; ATCC) was cultured in RPMI-1640 medium with 0.01 mg/mL bovine insulin (Life Technologies, Rockville, MD, USA). All media were supplemented with 100 IU/mL penicillin and 100 mg/mL

[6]To whom correspondence should be addressed.
E-mail: s0714@med.yokohama-cu.ac.jp

doi: 10.1111/cas.12196

streptomycin. Cells were incubated at 37°C in 5% CO_2 under humidified conditions.

Adenovirus vector construction. CRAd(Ad5/3-Cox2CRAd-ΔE3-ADP-Luc) has enhanced infectivity for pancreatic cancer cells as a result of a chimeric Ad5/3 fiber that consists of the tail and shaft of adenovirus serotype 5 with the knob of adenovirus serotype 3. Expression of E1A is under the control of the Cox2 promoter, and the luciferase gene is inserted adjacent to the *ADP* gene, which is in its native position despite a deletion in the E3. This CRAd was generated using homologous recombination in *Escherichia coli* as described previously (Fig. 1).[22–28] The recombinant virus was purified using an Adenovirus Purification kit (VIRAPUR, San Diego, CA, USA), and vp numbers were measured spectrophotometrically at an absorbance wavelength of 260 nm (vp = optical density 260 nm value × 10 (dilution rate) × 1.1 × 10^{12} viral particle /mL). The vectors were stored at −80°C until use. This genetic recombination was approved by the Ministry of Education, Culture, Sports, Science, and Technology of Japan.

***In vitro* luciferase assay.** Among pancreatic cancer cell lines, MiaPaCa-2 and Panc-1 express high levels of Cox2.[29] These cell lines were plated in 96-well black plates at a density of 1.0 × 10^4 cells/well, and infected with CRAd(Ad5/3-Cox2-CRAd-ΔE3-ADP-Luc) at 10 vp/well. Luciferase activity was analyzed daily for 7 days using an XFLUOR4 microplate reader (Tecan Japan, Kawasaki, Japan).

Effects of chemotherapeutic drugs estimated using *in vitro* MTT assays. The effects of chemotherapeutic drugs on MiaPaCa-2, Panc-1, and BxPC-3 cells were evaluated using MTT assays. The cell lines were plated into 96-well plates at a density of 2 × 10^4 cells/mL in 100 μL/well medium containing serum, and were allowed to grow for 24 h. An additional 100 μL medium containing 0.01 μg/mL GEM (Gemzar; Eli Lilley, Kobe, Japan) or 0.5 μg/mL tegafur/gimeracil/oteracil (TS-1; Taiho Pharmaceutical, Tokyo, Japan) was added. After 24, 48, 72, and 96 h, 20 μL/well MTT reagent (0.4% MTT; Sigma, St. Louis, MO, USA) with 0.1 M disodium succinate hexahydrate (Kanto Chemical, Tokyo, Japan) was added, and cells were incubated for a further 4 h. The formazans formed were dissolved in 150 μL DMSO (Kanto Chemical), and optical densities were read with an Elx800 Universal Microplate Reader (Bio-Tek Instruments, Winooski, VT, USA) at 590 nm.

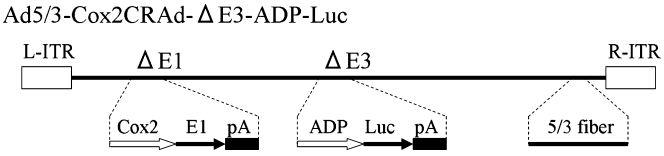

Fig. 1. Structure of the conditionally replicative adenovirus Ad5/3-Cox2CRAd-ΔE3-ADP-Luc. A chimeric Ad5/3 fiber enhances infectivity, a luciferase reporter gene is inserted at the E3 region deletion, and an adenovirus death protein (*ADP*) gene is in its native location. L-ITR, left inverted terminal repeat; R-ITR, right inverted terminal repeat.

***In vivo* detection of luciferase bioluminescence.** We needed to identify a pancreatic cancer cell line with high chemosensitivity that could easily be grafted. We therefore selected MiaPaCa-2 cells, which showed comparable GEM sensitivity to BxPC-3 cells and were more sensitive than Panc-1 cells (Fig. 2). In preliminary experiments, MiaPaCa-2 cells were also simple to graft.

We determined the time at which CRAd(Ad5/3-Cox2CRAd-ΔE3-ADP-Luc) replication peaked after the intratumoral injection of CRAds into MiaPaCa-2 xenografts by monitoring bioluminescence. Female BALB/c nu/nu mice (Charles River Laboratories, Yokohama, Japan) aged 5–7 weeks were injected s.c. on the right flank with 5.0 × 10^6 MiaPaCa-2 cells in 100 μL PBS. When tumors grew to 6–10 mm in diameter, they were injected intratumorally with 1.0 × 10^{10} vp CRAd (Ad5/3-Cox2CRAd-ΔE3-ADP-Luc) in 50 μL PBS. Previous studies have reported the effectiveness of CRAds as both cytocidal therapeutics and non-invasive imaging tools for tumors. In these studies, CRAds were injected intratumorally with 1.0 × 10^9–10^{10} vp in 50 μL PBS.[22–24,29] This injection volume is sufficient to infect the tumor safely, so we injected 1.0 × 10^{10} vp in 50 μL PBS. *In vivo* luciferase expression was assessed daily for 9 days by injecting each mouse i.p. with 150 mg/kg D-luciferin, and placing the animal in the imaging chamber of an IVIS 100 bioimaging system (Xenogen, Alameda, CA, USA). Images of the mice were captured and processed solely by adjusting the overall contrast and brightness using the IGOR Pro Imaging software (Xenogen).

***In vivo* use of CRAd(Ad5/3-Cox2CRAd-ΔE3-ADP-Luc) to monitor the pancreatic cancer cell response to GEM.** MiaPaCa-2 xenografts were established in 24 BALB/c nu/nu mice as described above. When the tumors grew to 4–6 mm in diameter (day 1), PBS was injected i.p. into group A mice (n = 12, untreated), and 1000 mg/kg GEM was injected i.p. into group B mice (n = 12, experimental) weekly. On days 19, 26, 33, and 40, 1.0 × 10^{10} vp CRAd(Ad5/3-Cox2CRAd-ΔE3-ADP-Luc) in 50 μL PBS was injected intratumorally into three mice in group A and three mice in group B. On days 22, 29, 36, and 43 (72 h after CRAd injection), the tumors in these mice were measured, their bioluminescence was imaged, and they were removed for *ex vivo* histopathology using H&E and Ki-67 staining. Gross tumor volume was calculated as $a \times b^2 \times 0.5$ mm^3, where a was the longest axis and b the shortest axis. Biolumines-

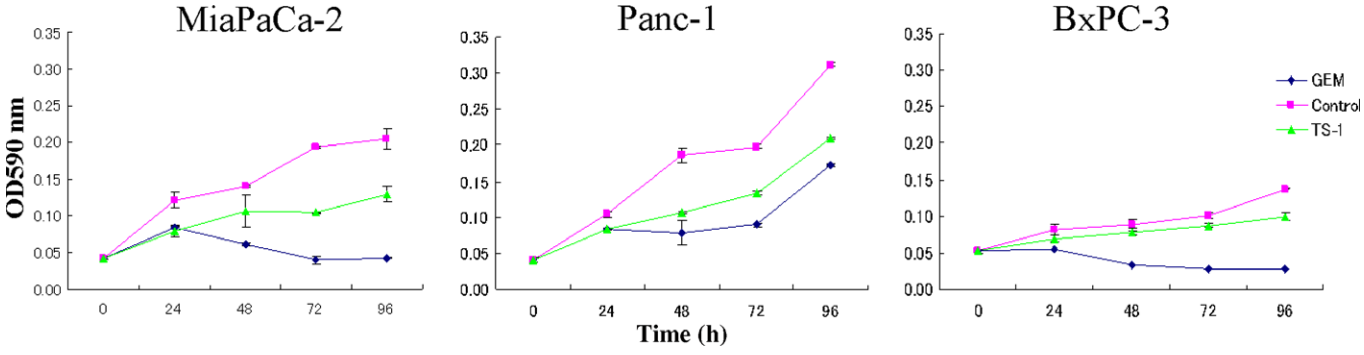

Fig. 2. Cytocidal effect of gemcitabine (GEM) and tegafur/gimeracil/oteracil (TS-1) on pancreatic cell lines. MiaPaCa-2, Panc-1, and BxPC-3 cells were plated into 96-well plates at 2 × 10^4 cells/mL in 100 μL serum-containing medium per well. After 24 h, an additional 100 μL medium containing 0.01 μg/mL GEM or 0.5 μg/mL TS-1 was added, and MTT assays were carried out after 24, 48, 72, and 96 h.

doi: 10.1111/cas.12196

cent values were measured using ROI analysis of the images collected, and correlations with gross tumor volume and the% viable tumor area were analyzed (Fig. 3). All experimental protocols involving live animals were approved by the Institutional Animal Care and Use Committee of Yokohama City University (Yokohama, Japan) and the National Cancer Center Research Institute (Tokyo, Japan).

Statistical analysis. Data from *in vitro* luciferase and MTT assays, and *in vivo* tumor volumes were expressed as means ± standard deviation. The statistical analysis of correlations between tumor volumes, percentage viability of tumors, and bioluminescence values was carried out using Pearson's correlation coefficient.

Results

***In vitro* characterization of pancreatic cell lines.** In the three pancreatic cell lines infected with CRAd(Ad5/3-Cox2CRAd-ΔE3-ADP-Luc), *in vitro* luciferase activity peaked on day 2 in Panc-1 cells at $1.0 \pm 0.05 \times 10^6$ RLU, on day 3 in MiaPaCa-2 cells at $8.6 \pm 0.4 \times 10^5$ RLU, and on day 4 in BxPC3 cells at $5.4 \pm 1.0 \times 10^5$ RLU (Fig. 4). The time course of luminescence appearance and the level reached were similar to those seen in the Cox2-positive, control cell line, A549, whereas no luminescence was seen in the Cox2-negative, negative control cell line, BT-474.

The effects of GEM and TS-1 on the pancreatic cell lines were assessed over 96 h in culture (Fig. 2). After 96 h, the absorbance at 590 nm was 0.04 ± 0.001 in wells treated with GEM, and 0.129 ± 0.01 in wells treated withTS-1, compared with 0.21 ± 0.01 in the control wells for MiaPaCa-2 cells. Similarly, for BxPC-3 cells after 96 h, the absorbance at 590 nm was 0.03 ± 0.004 in wells treated with GEM, and 0.1 ± 0.005 in wells treated with TS-1, compared with 0.14 ± 0.001 in untreated wells. By contrast, for Panc-1 cells, the absorbance at 590 nm was 0.172 ± 0.002 in wells treated with GEM, and 0.209 ± 0.002 in wells treated with TS-1, compared with 0.31 ± 0.002 in untreated wells. Thus, we identified GEM as an effective cytocidal agent, and MiaPaCa-2 and BxPC-3 cells as more sensitive to GEM than Panc-1 cells.

***In vivo* detection of luciferase bioluminescence.** After the intratumoral injection of CRAd(Ad5/3-Cox2CRAd-ΔE3-ADP-Luc) into MiaPaCa-2 xenografts on the flanks of BALB/c nu/nu mice, luciferase bioluminescence could be detected as early as the day after injection. As shown in Figure 5, bioluminescence peaked between days 3 and 7, and began to decrease by day 9.

***In vivo* evaluation of CRAd(Ad5/3-Cox2CRAd-ΔE3-ADP-Luc) for monitoring the response of pancreatic tumors to GEM.** As shown in Figure 6(a,b), in a representative individual from control group A mice, the s.c. tumor measured 12 mm on its major axis with an ROI of 1.1×10^7 total photon/s/cm^2/steradian by day 36 (Fig. 6a) and 13 mm on its major axis with an ROI of 1.7×10^7 p/s/cm^2/sr on day 43 (Fig. 6b). All cells were viable in the tumor, as shown by pathological examination of H&E and Ki-67 stained sections. For all mice in Group A, gross tumor volumes were 172.7 ± 33.0, 286.8 ± 46.9, 463.0 ± 97.25, and 842.0 ± 87.1 mm^3, and bioluminescence ROI values were 39.7 ± 9.0, 80.7 ± 15.7, 734.7 ± 259.9, and $1013.3 \pm 515.5 \times 10^4$ p/s/cm^2/sr on days 22, 29, 36, and 43, respectively. In all tumors from group A mice, cell viability was 100% at all time-points. As shown in Figure 6(c), there was a strong positive correlation between gross tumor volume and bioluminescence ($R = 0.94$).

In the example of a group B mouse treated with GEM, the s.c. tumor measured only 5 mm on the major axis, and the ROI of the tumor measured only 3.2×10^5 p/s/cm^2/sr on day 36 (Fig. 7a). On day 43, the s.c. tumor measured 5 mm on its major axis, the ROI of the tumor was 29 433 p/s/cm^2/sr, which was not significantly different to background, and no viable cells were detected (Fig. 7b). For all mice in Group B, tumor volumes were 47.5 ± 5.3, 37.3 ± 1.9, 44.8 ± 6.5, and 37.3 ± 1.9 mm^3, bioluminescence ROI values were 56.6 ± 9.1, 53.3 ± 8.1, 21.0 ± 4.3, and $0.02 \pm 0.004 \times 10^4$ p/s/cm^2/sr, and the% viable tumor area in the tumors was 72.7 ± 0.84, 67.0 ± 1.1, 44.3 ± 10.8, and 10.7 ± 7.5%, respectively, on days 22, 29, 36, and 43 (Fig. 7c). Although the mean gross tumor volume in these mice treated with GEM was stable after day 22 at approximately 40 mm^3, in contrast, the bioluminescence ROI values were still rapidly falling ($R = 0.31$). Furthermore, as the ROI values continued to fall, the% viable tumor area continued to fall and the measurements of CRAd bioluminescence and% viable tumor area were strongly correlated ($R = 0.96$), but not with gross tumor

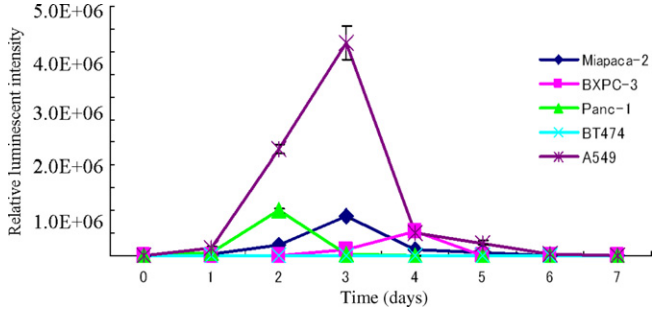

Fig. 4. Each cell line was infected with conditionally replicative adenovirus Ad5/3-Cox2CRAd-ΔE3-ADP-Luc at 10 viral particles per well. Luciferase activity was analyzed daily for 7 days.

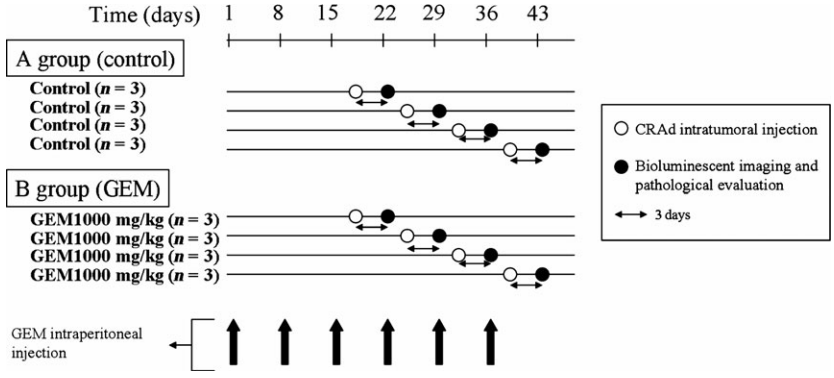

Fig. 3. Protocol for assessing the use of conditionally replicative adenovirus (CRAd), Ad5/3-Cox2CRAd-ΔE3-ADP-Luc, as an *in vivo* imaging diagnostic, showing the timing of i.p. gemcitabine (GEM) injection, intratumoral injection of CRAd, bioluminescent imaging, and *ex vivo* histopathology.

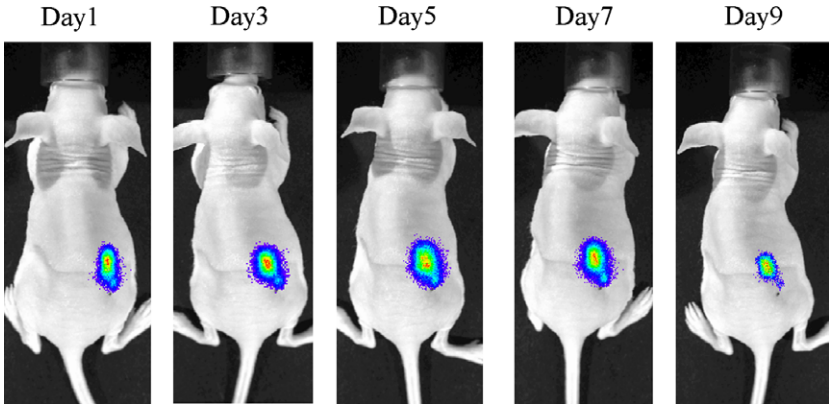

Fig. 5. Bioluminescent imaging of conditionally replicative adenovirus (CRAd) Ad5/3-Cox2CRAd-ΔE3-ADP-Luc replication after intratumoral injection into MiaPaCa-2 xenografts. BALB/c nu/nu mice were inoculated with MiaPaCa-2 cells, and when tumor nodules achieved a diameter of 6–10 mm, 1.0×10^{10} viral particles CRAd(Ad5/3-Cox2CRAd-ΔE3-ADP-Luc) were injected into tumors. The luciferase signal from the tumors was monitored from day 1.

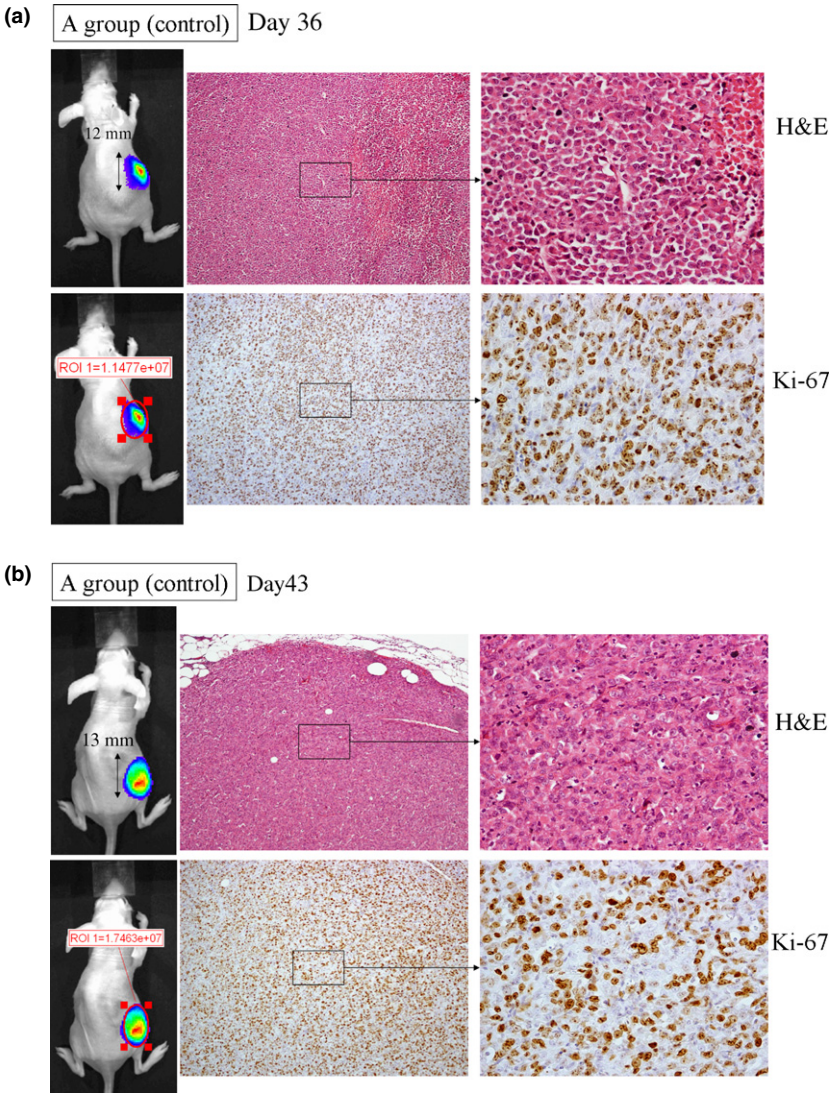

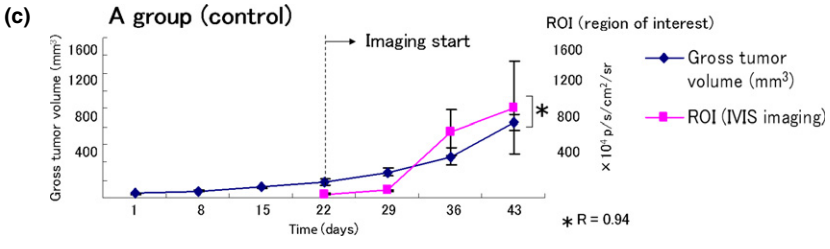

Fig. 6. Control results for the in vivo use of conditionally replicative adenovirus (CRAd) Ad5/3-Cox2CRAd-ΔE3-ADP-Luc to monitor the pancreatic cancer cell response to gemcitabine. Established MiaPaCa-2 xenografts in BALB/c nu/nu mice were injected i.p. with PBS weekly, then on days 33 (a) and 40 (b), 1.0×10^{10} viral particles CRAd(Ad5/3-Cox2CRAd-ΔE3-ADP-Luc) in 50 μL PBS were injected intratumorally. On day 36 (a) and day 42 (b), tumors (upper left panel) and bioluminescence were measured (lower left panel), and tumors were removed and stained with H&E (upper right panel) and Ki-67 (lower right panel). (c) Gross tumor volume and CRAd bioluminescence were closely correlated (R = 0.94).

doi: 10.1111/cas.12196

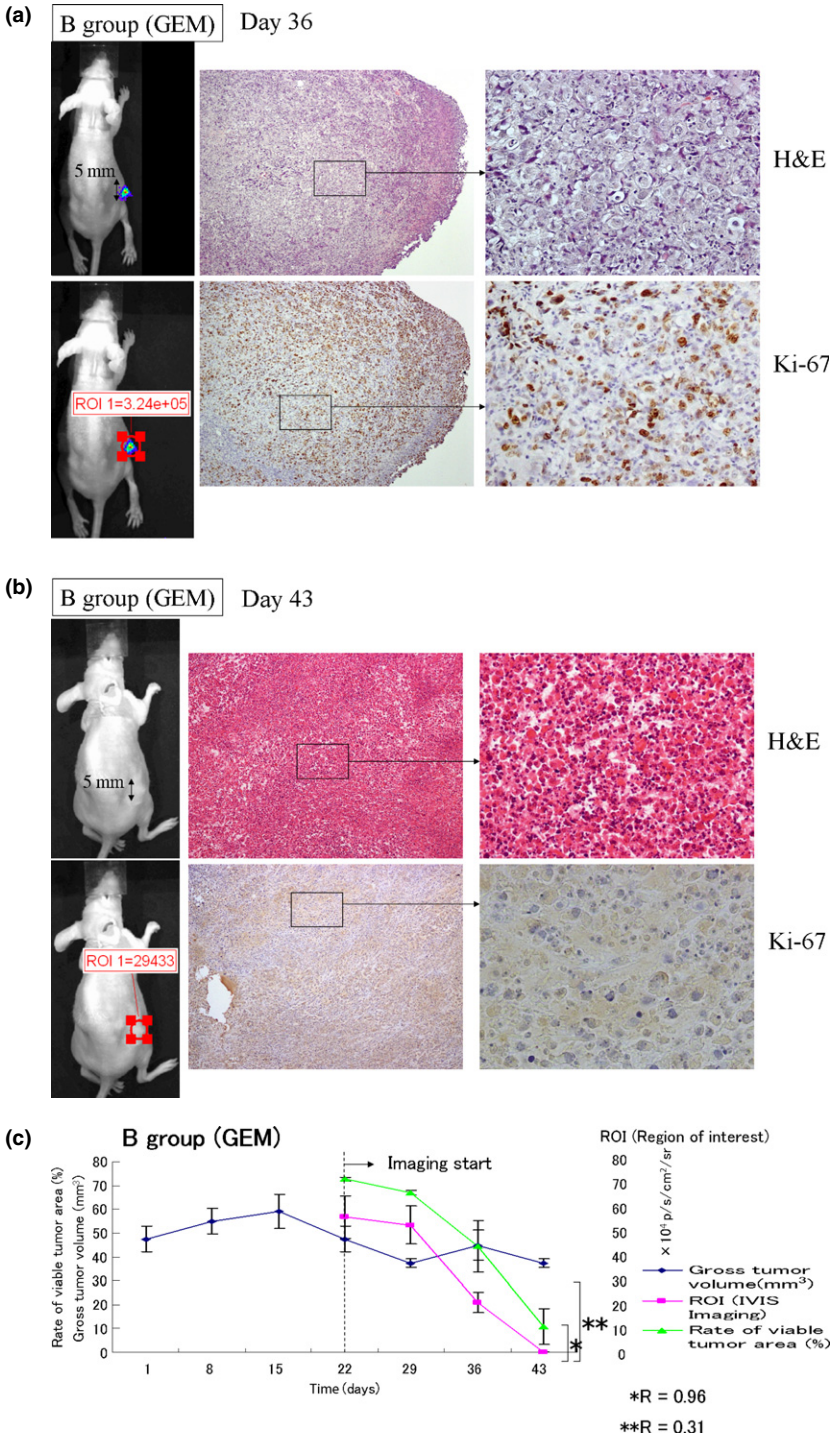

Fig. 7. *In vivo* use of conditionally replicative adenovirus (CRAd) Ad5/3-Cox2CRAd-ΔE3-ADP-Luc to monitor the pancreatic cancer cell response to gemcitabine. Established MiaPaCa-2 xenografts in BALB/c nu/nu mice were injected i.p. with gemcitabine weekly, then on days 33 (a) and 40 (b), 1.0×10^{10} viral particles CRAd(Ad5/3-Cox2CRAd-ΔE3-ADP-Luc) in 50 μL PBS were injected intratumorally. On day 36 (a) and day 42 (b), tumors (upper left panel) and bioluminescence were measured (lower left panel), and the tumors were removed and stained with H&E (upper right panel) and Ki-67 (lower right panel). (c) Xenograft growth was monitored by gross tumor volume, by% viable tumor area and CRAd bioluminescence. The correlations between these measurements were analyzed using Pearson's correlation coefficient. Bioluminescence correlated closely with% viable tumor area ($R = 0.96$) but not with gross tumor volume ($R = 0.31$).

volume. This suggested that CRAd bioluminescence might provide a more accurate measurement of tumor cell death than gross tumor volume.

Discussion

Previous studies have reported the effectiveness of CRAds as both cytocidal therapeutics and non-invasive imaging tools for tumors.[22–25,28] However, this is the first report to show the diagnostic ability of CRAds to image the effects of chemotherapy, using a CRAd with a Cox2 promoter, an E3 modification containing a bioluminescent reporter gene, an intact *ADP* gene, and a chimeric Ad5/3 fiber. In patients whose disease is stable after chemotherapy, it is difficult for current imaging techniques such as PET-CT to determine whether viable pancreatic cancer cells are still present in the nodule. If viable cells are histologically absent from a residual mass, then no bioluminescence will be emitted when the mass is imaged using CRAds. This imaging study found that even in residual masses of the same gross size, a CRAd could detect whether viable cancer cells were present in the residual mass.

In patients with pancreatic cancer, overall and disease-free survival times are significantly worse after R1 compared with R0 resections.[30] Recently, interest has increased in studying

the effect of neoadjuvant chemoradiation for patients with unresectable or borderline resectable pancreatic cancer, with the aim of making R0 resection a possibility. A systematic review of concurrent studies of neoadjuvant chemoradiation in primary unresectable pancreatic cancer found resection rates of 8–64%, and a surprisingly high rate of R0 resections with a median of 88%.[31] However, even after neoadjuvant chemoradiation, it is not uncommon for tumor surgical margins to be positive for cancer cells (0–44%) in postoperative histological examinations.[32–38] It is therefore important to distinguish any remaining cancer cells around major arteries, such as the celiac, superior mesenteric, and common hepatic arteries, from necrotic or fibrotic tissue present after neoadjuvant chemoradiotherapy.

Positron emission tomography–CT has a distinct advantage for identifying distant metastases in the whole body.[39] Heinrich *et al.*[40] reported 91% sensitivity and 64% specificity for PET-CT scanning for pancreatic cancer in 51 patients. They concluded that PET-CT represents an important staging method prior to resection of pancreatic cancer. However, PET-CT has difficulty detecting a tumor less than 1 cm in diameter because of its low spatial resolution.[41] Moreover, the rate of unexpected cancerous infiltrates in the superior mesenteric artery after neoadjuvant therapy not detected by PET-CT scans has been reported to be 28.5%.[42] Therefore, PET-CT scans appear useful for detecting distant metastases, but not as a decision-making method after chemotherapy and prior to surgery in patients with locally advanced pancreatic cancer abutting major vessels.

In a clinical setting, the grade classification of pathological response is based on the% viable tumor area after neoadjuvant chemotherapy. However, discrepancies between preoperative diagnosis and postoperative pathological response are problematic. Therefore, we used preoperative CRAds imaging to determine the% of viable tumor area rather than the% of viable tumor volume in this study. Using gross tumor volume, bioluminescence was found to correlate closely with the% viable tumor volume ($R = 0.93$), but not with the gross tumor volume ($R = 0.36$).

Clinically, if the gross tumor volume becomes large or small after neoadjuvant chemotherapy, the viable tumor area undergoes the same changes. However, if the gross tumor volume is stable after neoadjuvant chemotherapy, we cannot determine whether viable cells remain in the residual tumor. In such cases, CRAd imaging may be useful. As no other promising imaging tools are currently being considered for monitoring the effects of chemotherapy on locally advanced pancreatic cancer, the clinical application of CRAds is an important prospect.

In this study, CRAds were directly injected into tumors. It has been reported that CRAds injected directly into tumor infected not only primary tumors but also metastases in lymph nodes.[43] However, this technique is difficult unless patients undergo laparotomy. Endoscopic ultrasonography–fine needle aspiration biopsy has recently made remarkable progress. For example, the direct injection of immature dendritic cells into advanced pancreatic tumors using an EUS-guided fine-needle injection technique has been reported,[44] and CRAds could potentially be injected directly into pancreatic cancers using this method. Intravenously injected CRAds were also found to be safe in the infection of cancer cells and to replicate and emit light *in vivo*.[22,24,29] Although CRAd i.v. injection might be useful for hypervascular tumors such as pancreatic cancer, further studies are needed to investigate whether CRAds can successfully infect pancreatic tumors when administered by this route. Both intratumoral and i.v. delivery of CRAds could be clinically useful for imaging in the future.

Several different promoters have been used in association with adenoviral vectors, including Cox2 promoters in gastrointestinal cancers,[45–48] the midkine promoter in pediatric solid tumors,[49,50] ovarian cancer,[46] pancreatic cancer,[47] and cholangiocarcinoma,[48] the secretory leukocyte protease inhibitor promoter in ovarian cancer,[51,52] the vascular endothelial growth factor promoter and the gastrin-releasing peptide promoter in lung cancer and cholangiocarcinoma,[48,53] and the human telomerase reverse transcriptase promoter in gastric cancer,[54] breast cancer,[55] lung cancer,[56] prostate cancer,[21] colorectal cancer,[20,21] and hepatocellular carcinoma.[20,21] Modifications of the CRAd used in the present study with these tumor-specific promoters could therefore be evaluated for therapeutic use in other cancers.

For clinical applications involving the present study design, the important issues that need to be overcome include the safety of luciferin in humans, and the weakness of luciferase luminescence for use with CRAds in patients. Human sodium iodide symporter is a transmembrane glycoprotein that mediates the uptake of iodide into cells, and a CRAd vector expressing hNIS was recently reported.[57] This CRAd was transduced into prostate cancer cells and shown to induce functional hNIS expression, which increased radioisotope uptake and so mediated non-invasive tumor imaging using single photon-emission computed tomography – CT. This method could be applied to our CRAd vector by modifying it to express hNIS for an imaging system of higher sensitivity**.**

In this study, as we used the Cox2 promoter and a Cox2-positive cell line (MiaPaCa-2), all tumor cells became infected. However, in a clinical setting, Cox2-positive cells make up 90.0–90.4% of pancreatic cancers,[47,58] so approximately 1 in 10 cases of pancreatic cancer would be undetected. Therefore, it would be necessary to use EUS-FNA to examine protein overexpression individually. Although precision could be improved by modifying Cox2 to a protein that is detected, not all pancreatic cancers would express Cox2 or the detected protein so cell-negative populations would not be detected by CRAd leading to false negative results. The identification of an overexpressed protein common to all pancreatic cancer cells would overcome this problem.

In conclusion, this is the first study to our knowledge to focus on the diagnostic application of CRAds in assessing the effects of chemotherapy. Conditionally replicative adenovirus imaging could be a useful tool for evaluating pancreatic cancer infiltration into the celiac trunk or superior mesenteric artery after neoadjuvant chemotherapy, and to determine the effectiveness of neoadjuvant chemotherapy in down-staging pancreatic cancer for R0 surgical resection.

Acknowledgments

We thank Yasushi Ichikawa, Hirotoshi Akiyama, Hirochika Makino, Harumi Sakurada, Fumitaka Takeshita, Takahiro Ochiya, Tomoko Satake, and Yuka Honjoh for technical and secretarial assistance. This research was supported by Grants-in-Aid from the Japanese Ministry of Education, Culture, Sports, Science and Technology for Fundamental Research #20500395 (to C.K.) and #21791303 (to H.O.).

Disclosure Statement

The authors have no conflict of interest.

Abbreviations

ADP	adenovirus death protein
CRAd	conditionally replicative adenovirus
EUS-FNA	endoscopic ultrasonography–fine needle aspiration
FOLFORINOX	5-fluorouracil, leucovorin, irinotecan, and oxaliplatin
GEM	gemcitabine
hNIS	human sodium iodide symporter
PET-CT	positron emission tomography–computed tomography
RLU	relative light unit
ROI	region of interest
vp	viral particle

doi: 10.1111/cas.12196

References

1 Jemal A, Siegel R, Ward E *et al.* Cancer statistics, 2008. *CA Cancer J Clin* 2008; **58**: 71–96.
2 Gillen S, Schuster T, Meyer Zum Buschenfelde C, Friess H, Kleeff J Preoperative/neoadjuvant therapy in pancreatic cancer: a systematic review and meta-analysis of response and resection percentages. *PLoS Med* 2010; **7**: e1000267.
3 Neoptolemos JP, Stocken DD, Friess H *et al.* A randomized trial of chemoradiotherapy and chemotherapy after resection of pancreatic cancer. *N Engl J Med* 2004; **350**: 1200–10.
4 Neoptolemos JP, Stocken DD, Bassi C *et al.* Adjuvant chemotherapy with fluorouracil plus folinic acid vs gemcitabine following pancreatic cancer resection: a randomized controlled trial. *JAMA* 2010; **304**: 1073–81.
5 Oettle H, Post S, Neuhaus P *et al.* Adjuvant chemotherapy with gemcitabine vs observation in patients undergoing curative-intent resection of pancreatic cancer: a randomized controlled trial. *JAMA* 2007; **297**: 267–77.
6 Buchler MW, Wagner M, Schmied BM, Uhl W, Friess H, Z'Graggen K. Changes in morbidity after pancreatic resection: toward the end of completion pancreatectomy. *Arch Surg* 2003; **138**: 1310–4; discussion 5.
7 Cameron JL, Riall TS, Coleman J, Belcher KA. One thousand consecutive pancreaticoduodenectomies. *Ann Surg* 2006; **244**: 10–5.
8 Fernandez-del Castillo C, Rattner DW, Warshaw AL. Standards for pancreatic resection in the 1990s. *Arch Surg* 1995; **130**: 295–9; discussion 9-300.
9 Hartwig W, Hackert T, Hinz U *et al.* Multivisceral resection for pancreatic malignancies: risk-analysis and long-term outcome. *Ann Surg* 2009; **250**: 81–7.
10 Muller SA, Hartel M, Mehrabi A *et al.* Vascular resection in pancreatic cancer surgery: survival determinants. *J Gastrointest Surg* 2009; **13**: 784–92.
11 Tseng JF, Tamm EP, Lee JE, Pisters PW, Evans DB. Venous resection in pancreatic cancer surgery. *Best Pract Res Clin Gastroenterol* 2006; **20**: 349–64.
12 Hosein PJ, Macintyre J, Kawamura C *et al.* A retrospective study of neoadjuvant FOLFIRINOX in unresectable or borderline-resectable locally advanced pancreatic adenocarcinoma. *BMC Cancer* 2012; **12**: 199.
13 Conroy T, Desseigne F, Ychou M *et al.* FOLFIRINOX versus gemcitabine for metastatic pancreatic cancer. *N Engl J Med* 2011; **364**: 1817–25.
14 Strobel O, Berens V, Hinz U *et al.* Resection after neoadjuvant therapy for locally advanced, "unresectable" pancreatic cancer. *Surgery* 2012; **152**: S33–42.
15 Spaepen K, Stroobants S, Dupont P *et al.* [(18)F]FDG PET monitoring of tumour response to chemotherapy: does [(18)F]FDG uptake correlate with the viable tumour cell fraction? *Eur J Nucl Med Mol Imaging* 2003; **30**: 682–8.
16 Gomez-Navarro J, Curiel DT. Conditionally replicative adenoviral vectors for cancer gene therapy. *Lancet Oncol* 2000; **1**: 148–58.
17 Hecht JR, Bedford R, Abbruzzese JL *et al.* A phase I/II trial of intratumoral endoscopic ultrasound injection of ONYX-015 with intravenous gemcitabine in unresectable pancreatic carcinoma. *Clin Cancer Res* 2003; **9**: 555–61.
18 Schenk E, Essand M, Bangma CH *et al.* Clinical adenoviral gene therapy for prostate cancer. *Hum Gene Ther* 2010; **21**: 807–13.
19 Young A, McNeish IA. Oncolytic adenoviral gene therapy in ovarian cancer: why we are not wasting our time. *Future Oncol* 2009; **5**: 339–57.
20 Kishimoto H, Urata Y, Tanaka N, Fujiwara T, Hoffman RM. Selective metastatic tumor labeling with green fluorescent protein and killing by systemic administration of telomerase-dependent adenoviruses. *Mol Cancer Ther* 2009; **8**: 3001–8.
21 Kishimoto H, Zhao M, Hayashi K *et al.* In vivo internal tumor illumination by telomerase-dependent adenoviral GFP for precise surgical navigation. *Proc Natl Acad Sci USA* 2009; **106**: 14514–7.
22 Yamamoto M, Davydova J, Wang M, *et al.* Infectivity enhanced, cyclooxygenase-2 promoter-based conditionally replicative adenovirus for pancreatic cancer. *Gastroenterology* 2003; **125**: 1203–18.
23 Davydova J, Le LP, Gavrikova T, Wang M, Krasnykh V, Yamamoto M. Infectivity-enhanced cyclooxygenase-2-based conditionally replicative adenoviruses for esophageal adenocarcinoma treatment. *Cancer Res* 2004; **64**: 4319–27.
24 Armstrong L, Arrington A, Han J *et al.* Generation of a novel, cyclooxygenase-2-targeted, interferon-expressing, conditionally replicative adenovirus for pancreatic cancer therapy. *Am J Surg* 2012; **204**: 741–50.
25 Ono HA, Le LP, Davydova JG, Gavrikova T, Yamamoto M. Noninvasive visualization of adenovirus replication with a fluorescent reporter in the E3 region. *Cancer Res* 2005; **65**: 10154–8.
26 Chartier C, Degryse E, Gantzer M, Dieterle A, Pavirani A, Mehtali M. Efficient generation of recombinant adenovirus vectors by homologous recombination in *Escherichia coli*. *J Virol* 1996; **70**: 4805–10.
27 Krasnykh VN, Mikheeva GV, Douglas JT, Curiel DT. Generation of recombinant adenovirus vectors with modified fibers for altering viral tropism. *J Virol* 1996; **70**: 6839–46.
28 Davydova J, Gavrikova T, Brown EJ *et al.* In vivo bioimaging tracks conditionally replicative adenoviral replication and provides an early indication of viral antitumor efficacy. *Cancer Sci* 2010; **101**: 474–81.
29 Ramirez PJ, Vickers SM, Ono HA *et al.* Optimization of conditionally replicative adenovirus for pancreatic cancer and its evaluation in an orthotopic murine xenograft model. *Am J Surg* 2008; **195**: 481–90.
30 Zhang Y, Frampton AE, Cohen P *et al.* Tumor infiltration in the medial resection margin predicts survival after pancreaticoduodenectomy for pancreatic ductal adenocarcinoma. *J Gastrointest Surg* 2012; **16**: 1875–82.
31 Morganti AG, Massaccesi M, La Torre G *et al.* A systematic review of resectability and survival after concurrent chemoradiation in primarily unresectable pancreatic cancer. *Ann Surg Oncol* 2010; **17**: 194–205.
32 Snady H, Bruckner H, Cooperman A, Paradiso J, Kiefer L. Survival advantage of combined chemoradiotherapy compared with resection as the initial treatment of patients with regional pancreatic carcinoma. An outcomes trial. *Cancer* 2000; **89**: 314–27.
33 Sa Cunha A, Rault A, Laurent C *et al.* Surgical resection after radiochemotherapy in patients with unresectable adenocarcinoma of the pancreas. *J Am Coll Surg* 2005; **201**: 359–65.
34 Adhoute X, Smith D, Vendrely V *et al.* Subsequent resection of locally advanced pancreatic carcinoma after chemoradiotherapy. *Gastroenterol Clin Biol* 2006; **30**: 224–30.
35 Brunner TB, Grabenbauer GG, Kastl S *et al.* Preoperative chemoradiation in locally advanced pancreatic carcinoma: a phase II study. *Onkologie* 2000; **23**: 436–42.
36 Wilkowski R, Thoma M, Schauer R, Wagner A, Heinemann V. Effect of chemoradiotherapy with gemcitabine and cisplatin on locoregional control in patients with primary inoperable pancreatic cancer. *World J Surg* 2004; **28**: 1011–8.
37 Wilkowski R, Thoma M, Bruns C Wagner A, Heinemann V. Chemoradiotherapy with gemcitabine and continuous 5-FU in patients with primary inoperable pancreatic cancer. *JOP* 2006; **7**: 349–60.
38 Lind PA, Isaksson B, Almstrom M, *et al.* Efficacy of preoperative radiochemotherapy in patients with locally advanced pancreatic carcinoma. *Acta Oncol* 2008; **47**: 413–20.
39 Izuishi K, Yamamoto Y, Sano T, Takebayashi R, Masaki T, Suzuki Y. Impact of 18-fluorodeoxyglucose positron emission tomography on the management of pancreatic cancer. *J Gastrointest Surg* 2010; **14**: 1151–8.
40 Heinrich S, Goerres GW, Schafer M *et al.* Positron emission tomography /computed tomography influences on the management of resectable pancreatic cancer and its cost-effectiveness. *Ann Surg* 2005; **242**: 235–43.
41 Gambhir SS, Shepherd JE, Shah BD *et al.* Analytical decision model for the cost-effective management of solitary pulmonary nodules. *J Clin Oncol* 1998; **16**: 2113–25.
42 Patel M, Hoffe S, Malafa M *et al.* Neoadjuvant GTX chemotherapy and IMRT-based chemoradiation for borderline resectable pancreatic cancer. *J Surg Oncol* 2011; **104**: 155–61.
43 Kojima T, Watanabe Y, Hashimoto Y *et al.* In vivo biological purging for lymph node metastasis of human colorectal cancer by telomerase-specific oncolytic virotherapy. *Ann Surg* 2010; **251**: 1079–86.
44 Nakamura I, Kanazawa M Sato Y *et al.* Clinical evaluation of dendritic cells vaccination for advanced cancer patients at Fukushima Medical University. *Fukushima J Med Sci* 2012; **58**: 40–8.
45 Yamamoto M, Alemany R, Adachi Y, Grizzle WE, Curiel DT. Characterization of the cyclooxygenase-2 promoter in an adenoviral vector and its application for the mitigation of toxicity in suicide gene therapy of gastrointestinal cancers. *Mol Ther* 2001; **3**: 385–94.
46 Casado E, Gomez-Navarro J, Yamamoto M, *et al.* Strategies to accomplish targeted expression of transgenes in ovarian cancer for molecular therapeutic applications. *Clin Cancer Res* 2001; **7**: 2496–504.
47 Wesseling JG, Yamamoto M, Adachi Y *et al.* Midkine and cyclooxygenase-2 promoters are promising for adenoviral vector gene delivery of pancreatic carcinoma. *Cancer Gene Ther* 2001; **8**: 990–6.
48 Nagi P, Vickers SM, Davydova J *et al.* Development of a therapeutic adenoviral vector for cholangiocarcinoma combining tumor-restricted gene expression and infectivity enhancement. *J Gastrointest Surg* 2003; **7**: 364–71.
49 Adachi Y, Reynolds PN, Yamamoto M *et al.* Midkine promoter-based adenoviral vector gene delivery for pediatric solid tumors. *Cancer Res* 2000; **60**: 4305–10.
50 Adachi Y, Reynolds PN, Yamamoto M *et al.* A midkine promoter-based conditionally replicative adenovirus for treatment of pediatric solid tumors and bone marrow tumor purging. *Cancer Res* 2001; **61**: 7882–8.
51 Barker SD, Coolidge CJ, Kanerva A, *et al.* The secretory leukoprotease inhibitor (SLPI) promoter for ovarian cancer gene therapy. *J Gene Med* 2003; **5**: 300–10.
52 Barker SD, Dmitriev IP, Nettelbeck DM *et al.* Combined transcriptional and transductional targeting improves the specificity and efficacy of adenoviral gene delivery to ovarian carcinoma. *Gene Ther* 2003; **10**: 1198–204.
53 Inase N, Horita K, Tanaka M, Miyake S, Ichioka M, Yoshizawa Y. Use of gastrin-releasing peptide promoter for specific expression of thymidine kinase gene in small-cell lung carcinoma cells. *Int J Cancer* 2000; **85**: 716–9.
54 Ito H, Inoue H, Sando N *et al.* Prognostic impact of detecting viable circulating tumour cells in gastric cancer patients using a telomerase-specific viral agent: a prospective study. *BMC Cancer* 2012; **12**: 346.

55 Kim SJ, Masago A, Tamaki Y *et al.* A novel approach using telomerase-specific replication-selective adenovirus for detection of circulating tumor cells in breast cancer patients. *Breast Cancer Res Treat* 2011; **128**: 765–73.
56 Liu D, Kojima T, Ouchi M *et al.* Preclinical evaluation of synergistic effect of telomerase-specific oncolytic virotherapy and gemcitabine for human lung cancer. *Mol Cancer Ther* 2009; **8**: 980–7.
57 Oneal MJ, Trujillo MA, Davydova J, McDonough S, Yamamoto M, Morris JC III. Characterization of infectivity-enhanced conditionally replicating adenovectors for prostate cancer radiovirotherapy. *Hum Gene Ther* 2012; **23**: 951–9.
58 Tucker ON, Dannenberg AJ, Yang EK *et al.* Cyclooxygenase-2 expression is upregulated in human pancreatic cancer. *Cancer Res* 1999; **59**: 987–90.

doi: 10.1111/cas.12196